

NEUTRINO FACTORY NEAR DETECTOR SIMULATION

YORDAN KARADZHOV, ROUMEN TSENOV

*Department of Atomic Physics,
Faculty of Physics, St. Kliment Ohridski University of Sofia*

Йордан Караджов, Румен Ценов. СИМУЛИРАНЕ НА БЛИЗКИЯ ДЕТЕКТОР НА НЕУТРИННА ФАБРИКА

Ускорителен комплекс, наречен неутринна фабрика, базиран на магнитни натрупващи пръстени за мюони, е един от инструментите с най-добри качества за изучаване на осцилациите на неутрината, включително и за евентуалното наблюдаване на CP-нарушение в лептонния сектор на Стандартния модел на частиците и взаимодействията. В настоящата работа ние представяме резултатите от симулационни пресмятания за възможния брой чисто лептонни процеси $\nu_\mu + e^- \rightarrow \nu_e + \mu^-$ и разсейвания върху нуклони $\nu_\mu + N \rightarrow \mu^- + X$, които биха могли да се наблюдават в т.нар. близък детектор на неутринната фабрика. Целта е чрез наблюдаване на първия процес и потискане на фона от втория процес да бъде определен потокът неутрино от неутринната фабрика. Разгледан е набор от експериментално измерими величини и е изследвано нивото на разделяне, което може да се постигне чрез използването им.

Yordan Karadzhov, Roumen Tsenov. NEUTRINO FACTORY NEAR DETECTOR SIMULATION

A neutrino factory based on a muon storage ring is the ultimate tool for studies of neutrino oscillations, including possibly the discovery of leptonic CP violation. We present a simulation of the neutrino factory baseline near detector interaction rates for the purely leptonic process $\nu_\mu + e^- \rightarrow \nu_e + \mu^-$ and for $\nu_\mu + N \rightarrow \mu^- + X$ scattering in view of measuring the first one and suppressing the second one for neutrino flux estimation. A set of most sensitive measurable quantities are discussed and their selective power against experimental uncertainties is examined.

Keywords: neutrino factory, near detector, neutrino flux measurement, leptonic interactions

PACS numbers: 07.77.Ka; 13.35.Bv; 13.66.-a; 14.60.Ef; 14.60.Lm

For contacts: Yordan Karadzhov, Department of Atomic Physics, St. Kliment Ohridski University of Sofia, 5 J. Bourchier blvd, Sofia, BG-1164, tel:+35928161850, fax:+35929622546, E-mail: yordan@phys.uni-sofia.bg.

1. INTRODUCTION

The *neutrino factory* [1] [2] (Fig. 1) is a possible future particle accelerator facility dedicated to make detailed studies of the phenomenon of neutrino oscillations [3]. The *neutrino factory* creates very intense beams of neutrinos produced by decays of muons $\mu^- \rightarrow e^- + \nu_e + \nu_\mu$ or $\mu^+ \rightarrow e^+ + \nu_e + \nu_\mu$ in storage rings. The neutrino beams are intense enough to produce high detection rates even on the opposite side of the Earth in the so called *far detector*. This will be used to make precise measurements of the parameters describing neutrino oscillations and CP-violation for leptons.

In order to perform measurements of neutrino oscillations at a neutrino facility, it is necessary to establish the ratio of neutrino interactions. The aim of the so called *near detector* of the *neutrino factory* is to measure precisely the absolute neutrino flux, the neutrino cross sections and to estimate the background to the *far detector*. Hence, the careful design of the near detector is crucial for the reduction the long baseline neutrino oscillation systematic errors [4].

In this note we will show how the inverse muon decay reaction can be used to measure the neutrino flux coming from the *neutrino factory* storage ring, provided that the resolution in hadronic energy E_{had} can be determined down to tens of MeV. Discrimination power of several experimentally measurable variables (e.g. muon scattering angle θ_μ , scattered muon energy E_μ , recoil (hadronic) energy E_{had} and the composite variable $E_\mu * \theta_\mu^2$ to distinguish the inverse muon decay reaction from charged current neutrino scattering off target nucleons has been examined.

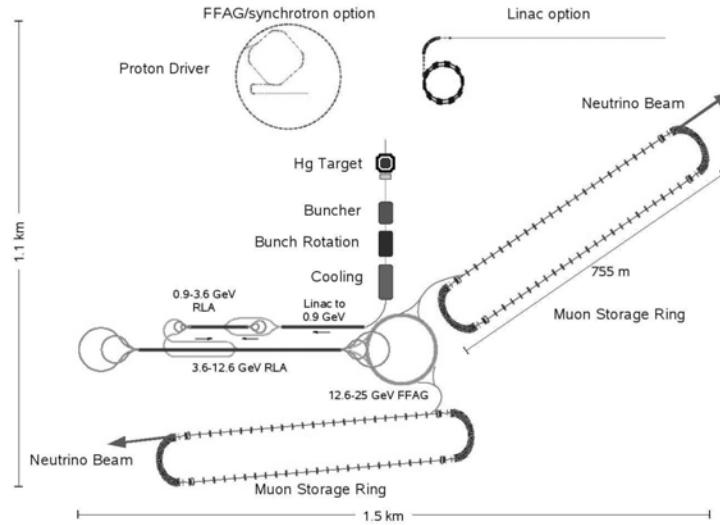


Fig. 1. Neutrino Factory scheme

2. SIMULATION OF THE NEUTRINO BEAM AT THE NEAR DETECTOR

In the muon decay, the probability for having a neutrino with a given energy and polar angle in the rest system of the muon is proportional to the following expressions:

$$\text{for } \nu_\mu : \frac{d^2N}{dx d\Omega} \sim ((3-2x) + \cos P_\mu(1-2x))x^2, \quad (1)$$

$$\text{for } \nu_{\bar{e}} : \frac{d^2N}{dx d\Omega} \sim ((1-x) + \cos P_\mu(1-x))x^2, \quad (2)$$

where $x = 2E_\nu/m_\mu$, P_μ is the polarization of the muon and θ is the angle between the polarization vector and the direction of the neutrino [5], see also Fig. 2.

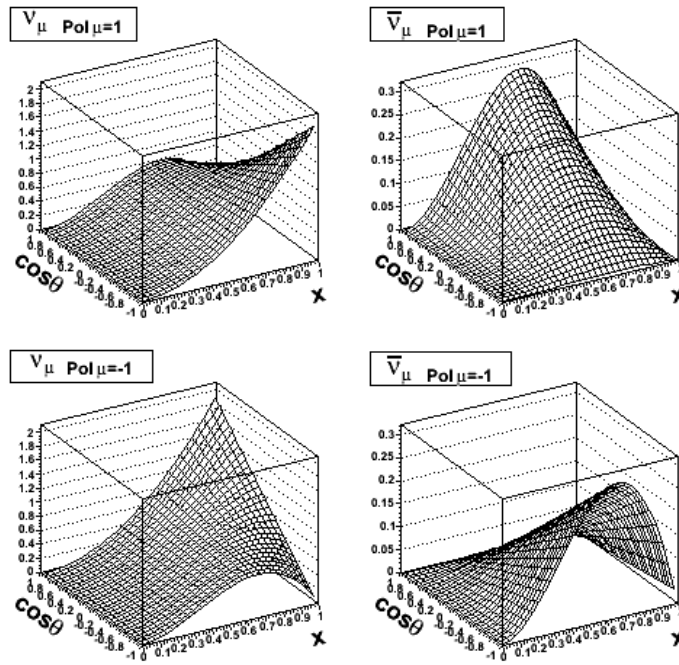


Fig. 2. Muon decay matrix elements for the two possible polarizations of the muon

In order to estimate the neutrino flux at the position of the *near detector* a Monte Carlo simulation of the muon decays in the storage ring has been developed. In the simulation we use the following input parameters of the muon beam defined

as a baseline set of options by the International Design Study for Neutrino Factory Committee [6]:

- length of the straight section of the muon storage ring: 600 m;
- muon beam energy: 25 GeV ;
- muon beam energy distribution: Gaussian ($\sigma = 80$ MeV);
- muon beam angular distribution: Gaussian ($\sigma = 0.5$ mrad);
- position of the near detector: 100 m after the end of the straight section,

The most important properties of the neutrino beam are illustrated in Fig. 3, 4 and 5. Fig. 3 shows the distributions of neutrino energy versus the polar angle for the two neutrino flavors and for the two possible polarizations of the decaying muons.

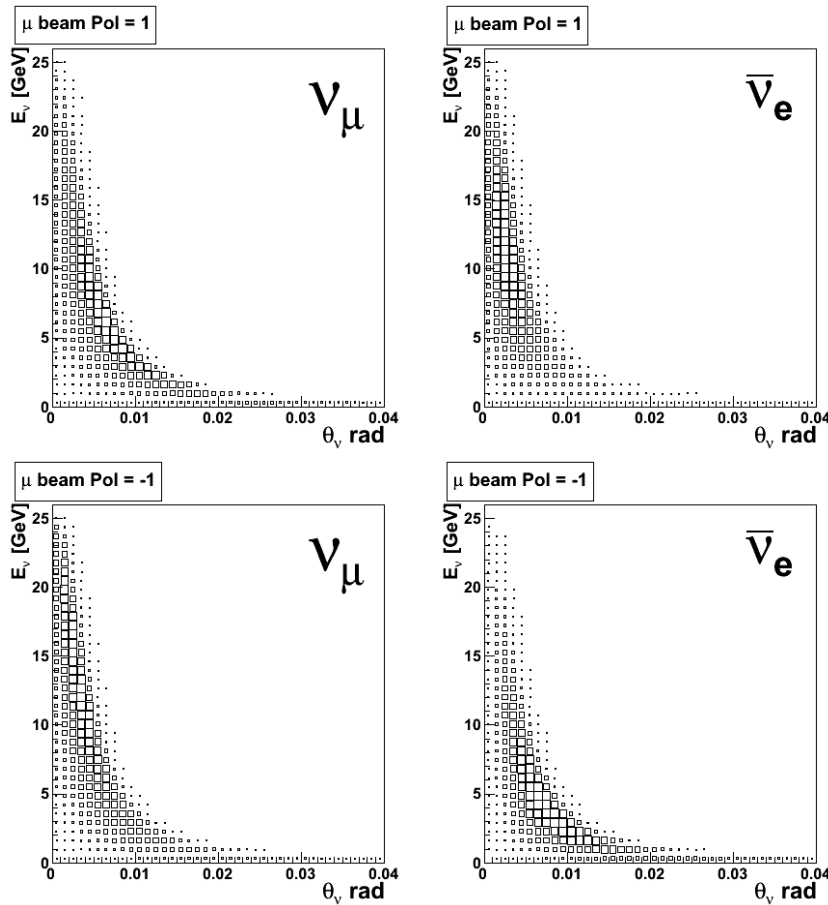


Fig. 3. Distributions of the neutrinos over their energy and polar angle at the position of the near detector for the two polarizations of the decaying muons

The profile of the neutrino beam at 100 m after the end of the straight section of the muon storage ring is shown in Fig. 4. The flux depends on the polarization of the muon beam. This is illustrated in Fig. 5, where the neutrino flux in neutrinos/cm² is shown as a function of the distance from the beam axis.

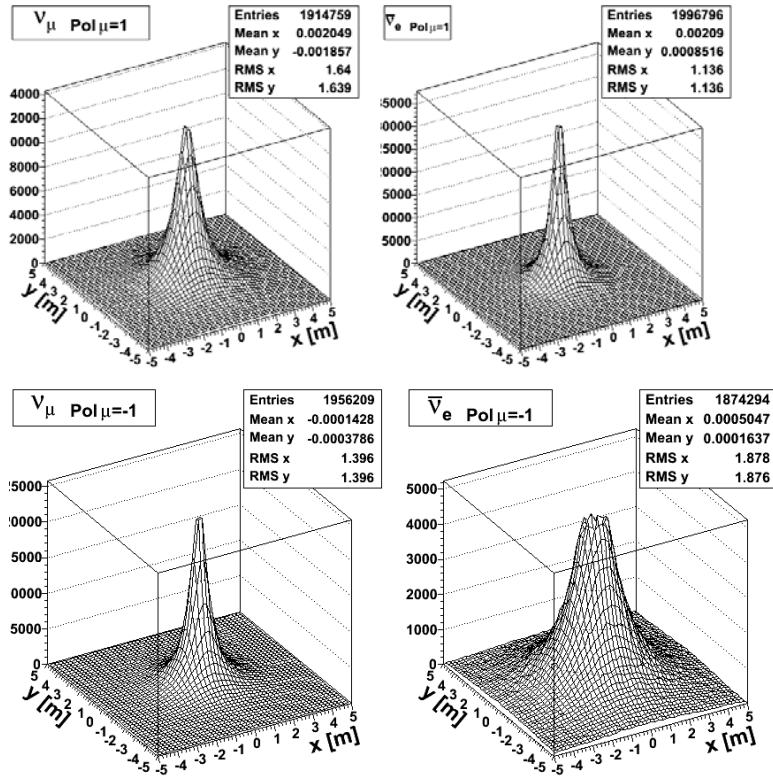


Fig. 4. Transversal profiles of the neutrino beams at the position of the near detector for the two polarizations of the decaying muons

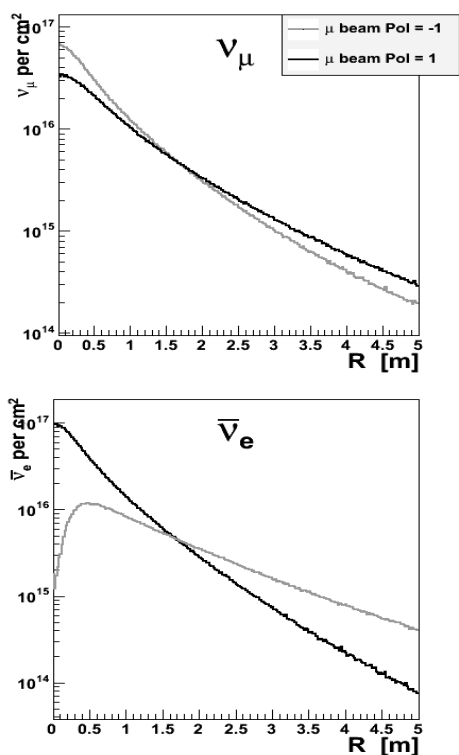


Fig. 5. The neutrino flux (neutrinos/cm²) for ν_μ (upper panel) and ν_e (lower panel) in a plane perpendicular to the beam axis at the position of the near detector for the two indicated polarizations of the decaying muons

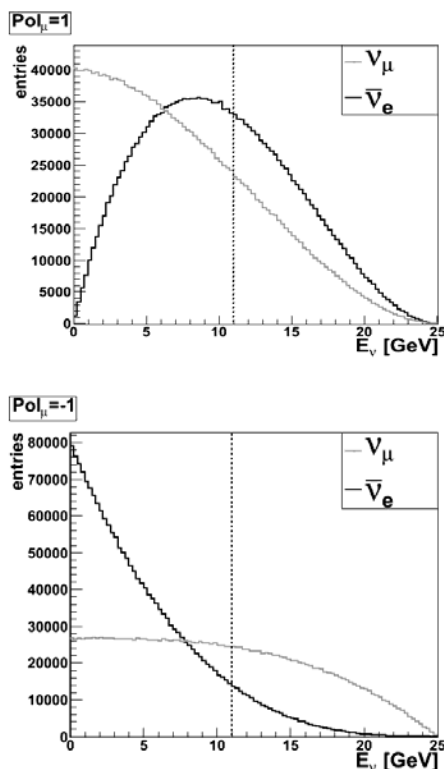


Fig. 6. Distributions over the neutrino energy for the two polarizations of the decaying muons. Dotted lines indicate the threshold for the leptonic processes

3. MEASUREMENT OF THE NEUTRINO FLUX IN THE NEAR DETECTOR

The quasielastic scattering off electrons can be used to measure the flux, because its absolute cross-section can be calculated theoretically with enough confidence. The two pure leptonic interactions with matter of neutrinos from μ -decay are:

$$\nu_\mu + e^- \rightarrow \nu_e + \mu^- \quad (3)$$

and

$$\bar{\nu}_e + e^- \rightarrow \bar{\nu}_\mu + \mu^- \quad (4)$$

For the process (3) the cross section is isotropic in the c.m. system and is given by

$$\sigma = \frac{G_F^2 (s - m_\mu^2)^2}{\pi s}, \quad (5)$$

where s is the invariant mass of the system, G_F is the Fermi constant of the weak interactions and m_μ is the mass of the muon.

For the process (4) the differential cross section in the c.m. system is given by

$$\sigma = \frac{G_F^2 (s - m_\mu^2)^2}{\pi s} \times \left(1 + \frac{s - m_\mu^2}{s + m_\mu^2} \cos \theta\right) \left(1 + \frac{s - m_e^2}{s + m_e^2} \cos \theta\right) \quad (6)$$

and the total cross section is:

$$\sigma = \frac{G_F^2 (s - m_\mu^2)^2}{\pi s} \left(E_e E_\mu + \frac{1}{3} E_{\bar{\nu}_\mu} E_{\bar{\nu}_e}\right), \quad (7)$$

where $E_{\bar{\nu}_\mu}$ and $E_{\bar{\nu}_e}$ are the energies of the neutrinos in the c.m. system,

$$E_{\bar{\nu}_\mu} = \frac{s - m_\mu}{2\sqrt{s}}, \quad (8)$$

$$E_{\bar{\nu}_e} = \frac{s - m_e}{2\sqrt{s}} \quad (9)$$

They depend on s only. Both processes have a threshold at ~ 11 GeV. The full energy spectra of the beam neutrinos are shown in Fig.6, where the threshold for the two processes (3) and (4) is shown with dotted line.

However, the energy spectra of neutrinos that cross the detector are different because of the constraint in the solid angle. If we consider a cylindrical detector with radius of 1.5 m, the energy spectra of the beam neutrinos that cross the detector are shown in Fig. 7. Again the dotted line indicates the threshold for the leptonic processes.

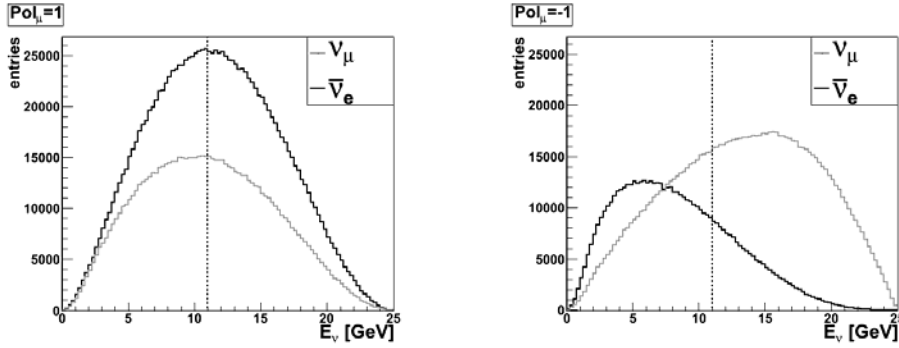


Fig. 7. Distributions over the neutrino energy at the position of the near detector for the two polarizations of the decaying muons. Dotted lines indicate the threshold for the leptonic processes

By using the characteristics of the neutrinos generated in the simulation of the neutrino beam we have simulated the leptonic processes (3) and (4). For the muons generated in the detector the two-dimensional distributions over the muon energy and its scattering angle are shown on Fig. 8. Distributions for the two leptonic processes and for the two possible polarizations of the decaying muons are shown. Fig. 9 shows the one-dimensional distributions over the energy and the scattering angle of the muons generated in the detector. Again they are for the two leptonic processes and for the two possible polarizations of the decaying muons.

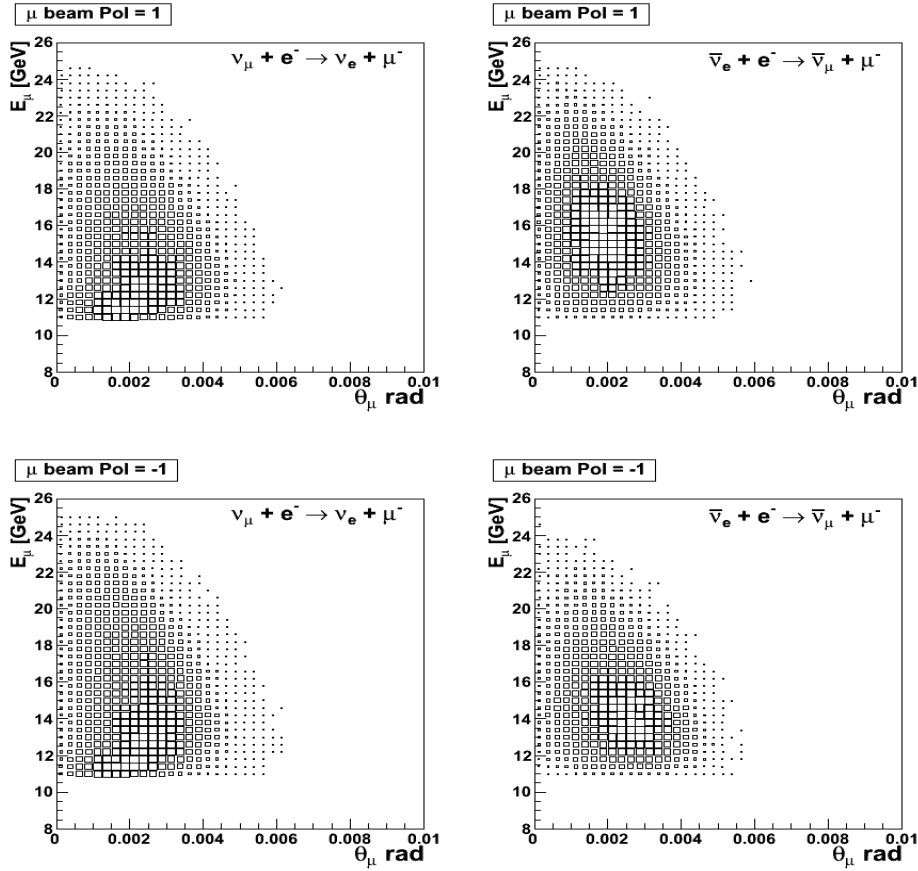


Fig. 8. Distributions over the energy and polar angle of the muons generated in the indicated reactions for the two polarizations of the decaying muons

If we want to measure the neutrino flux by using the quasi-elastic scattering off electrons (for earlier measurements of these processes see [7, 8]), the detector has to be able to distinguish between the leptonic events (processes (3) and (4)) and

inclusive charged-current (CC) neutrino interactions with nucleus $\nu_\mu + N \rightarrow \mu^- + X$, which are a few orders of magnitude more intensive.

In order to test different criteria for suppression of the background from these CC reactions we make use of the neutrino event generator GENIE [9, 10] to simulate the interactions of the neutrinos with a cylindrical detector, 5 m long and with radius of 1.5 m, made of polystyrene ($\rho = 1.032 \text{ g/cm}^3$). The following neutrino interaction processes are included in the GENIE event generator:

- quasi-elastic scattering;
- elastic neutral-current scattering;
- baryon resonance production in charged and neutral current interactions;
- coherent neutrino-nucleus scattering;
- non-resonant deep inelastic scattering (DIS);
- quasi-elastic charm production;
- deep-inelastic charm production;
- neutrino-electron elastic scattering;
- inverse muon decay.

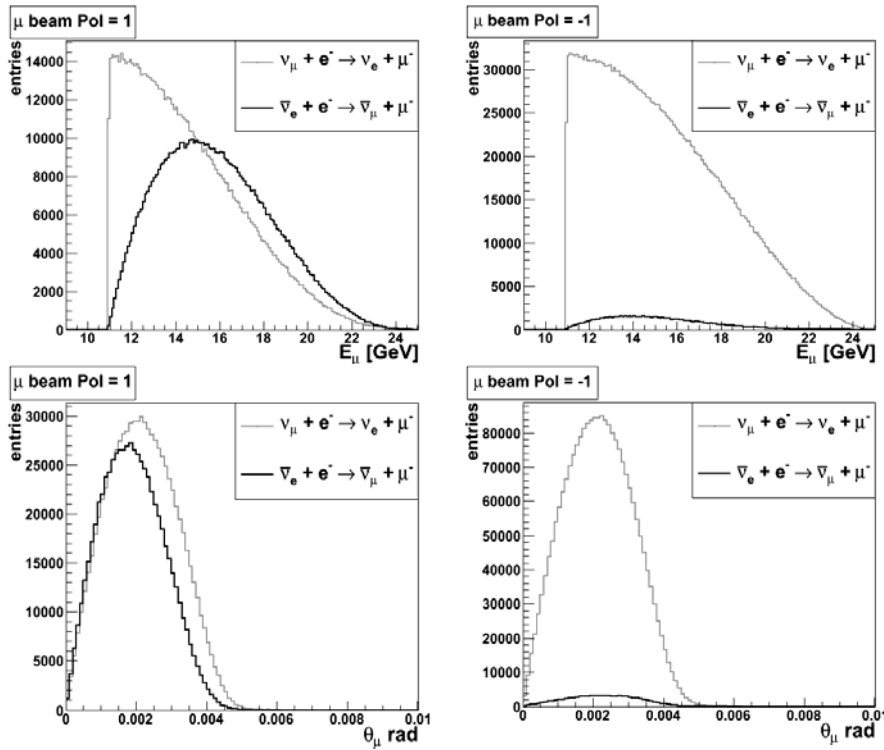


Fig. 9. The energy (top) and polar angle distributions (bottom) of the muons generated in the detector by the indicated reactions for the two polarizations of the decaying muons

We consider unpolarized muon beam in the storage ring, namely equal amounts of muons with polarization $+1$ and -1 . For such a polarization of the beam the process (4) (which is not included in GENIE) is ~ 10 times less intensive than process (3). The results below correspond to statistic of $\sim 3 \times 10^{17}$ muon decays in the storage ring (approx. 5 hours of work of the Neutrino Factory). Fig. 10 demonstrates the dependence of the leptonic event rate on the distance from the straight section end and Fig. 11 represents the variation with the distance from the beam axis. Kinematical distributions of the background νN events are demonstrated on Fig. 12 and Fig. 13.

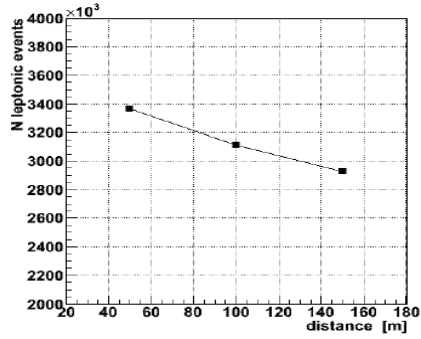


Fig. 10. Number of leptonic events as a function of the distance from the straight section end

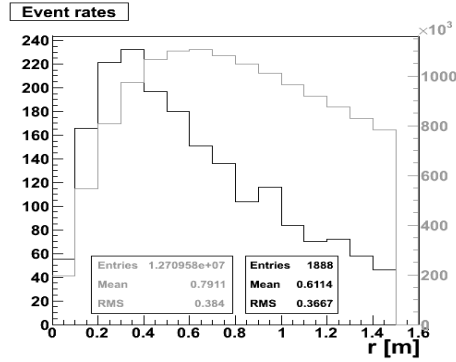


Fig. 11. Number of leptonic events (black, left scale) and inclusive charged-current events (gray, right scale) at the position of the near detector as a function of the distance from the beam axis

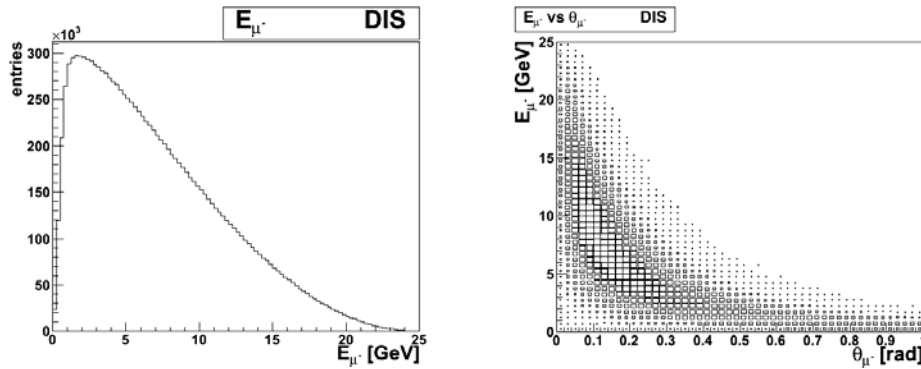


Fig. 12. Distributions over energy and polar angle of the muons generated in the detector in the inclusive reactions νN (right panel). Projection of the same distribution on the E_μ axis is shown on the left panel

It is considered also that the detector will be able to measure the angle between the beam axis and the direction of the outgoing muon θ_μ , the momentum of the outgoing muon, thus the energy E_μ , the transverse momentum p_T , and the total recoil (hadronic) energy E_{had} .

Several scenarios for the detector resolutions have been adopted:

- poor resolutions:

$$\sigma(\theta_\mu) = 1.0 \text{ mrad}; \quad \sigma(E_\mu)/E_\mu = 10\%; \quad \sigma(E_{\text{had}})/E_{\text{had}} = 10\%; \quad (10)$$

- medium resolutions:

$$\sigma(\theta_\mu) = 0.5 \text{ mrad}; \quad \sigma(E_\mu)/E_\mu = 5\%; \quad \sigma(E_{\text{had}})/E_{\text{had}} = 5\%; \quad (11)$$

- best resolutions:

$$\sigma(\theta_\mu) = 0.1 \text{ mrad}; \quad \sigma(E_\mu)/E_\mu = 1\%; \quad \sigma(E_{\text{had}})/E_{\text{had}} = 1\%. \quad (12)$$

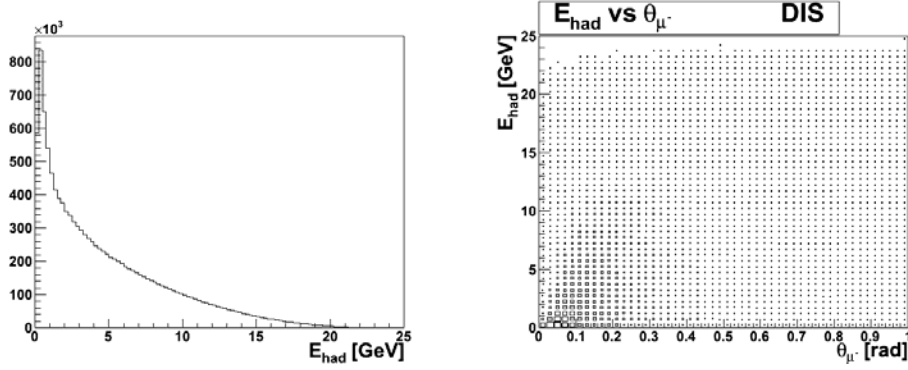


Fig. 13. Distribution over recoil (hadronic) energy and scattering angle of the muons generated in the detector in the inclusive reactions νN (right panel). Projection of the same distribution on the E_{had} axis is shown on the left panel

Different variables for suppression of the background from inclusive νN CC reactions have been examined:

- muon scattering angle θ_μ ;
- transverse momentum p_T ;
- $E_\mu * \theta_\mu^2$;
- recoil (hadronic) energy E_{had} .

Spectra of the events over smeared θ_μ and $E_\mu * \theta_\mu^2$ for *poor* and *best* resolutions scenario and for cuts on the recoil energy depicted on Fig. 14 are shown on Fig. 15 and Fig. 16. The obtained results for the different scenarios and when exploiting different suppression variables are summarized in Table 1.

Table 1. Summary of the results for signal and background estimation in the different scenarios. The number of generated leptonic events in the *near detector* was 1888

Scenarios	Cut on	Number of all events below the cut	Number of the background events	Number of the background events as obtained from the fit
best, $E_{\text{had}} < 100$ MeV	θ_μ	2476	601	455 ± 53
best, $E_{\text{had}} < 100$ MeV	$E_\mu * \theta_\mu^2$	2725	838	1127 ± 26
best, $E_{\text{had}} < 200$ MeV	θ_μ	4614	2739	3144 ± 158
best, $E_{\text{had}} < 200$ MeV	$E_\mu * \theta_\mu^2$	5826	3939	4840 ± 52
best, $E_{\text{had}} < 300$ MeV	θ_μ	6217	4342	4192 ± 177
best, $E_{\text{had}} < 300$ MeV	$E_\mu * \theta_\mu^2$	8097	6210	7541 ± 64
medium, $E_{\text{had}} < 100$ MeV	θ_μ	2458	611	468 ± 56
medium, $E_{\text{had}} < 100$ MeV	$E_\mu * \theta_\mu^2$	2724	843	1129 ± 26
medium, $E_{\text{had}} < 200$ MeV	θ_μ	4633	2786	3159 ± 159
medium, $E_{\text{had}} < 200$ MeV	$E_\mu * \theta_\mu^2$	5842	3961	4858 ± 52
medium, $E_{\text{had}} < 300$ MeV	θ_μ	6244	4397	4257 ± 177
medium, $E_{\text{had}} < 300$ MeV	$E_\mu * \theta_\mu^2$	8164	6283	7575 ± 64
poor, $E_{\text{had}} < 100$ MeV	θ_μ	2424	642	587 ± 64
poor, $E_{\text{had}} < 100$ MeV	$E_\mu * \theta_\mu^2$	2726	893	1196 ± 26
poor, $E_{\text{had}} < 200$ MeV	θ_μ	4686	2904	3172 ± 159
poor, $E_{\text{had}} < 200$ MeV	$E_\mu * \theta_\mu^2$	5946	4109	4969 ± 52
poor, $E_{\text{had}} < 300$ MeV	θ_μ	6381	4599	4288 ± 177
poor, $E_{\text{had}} < 300$ MeV	$E_\mu * \theta_\mu^2$	8357	6524	7701 ± 66

It is seen that, by imposing suitable cut on the recoil energy and subtracting the fitted inclusive background under the peak, it is possible to determine statistically the number of events due to pure leptonic scattering with a precision of a few percent. Both variables θ_μ and $E_\mu * \theta_\mu^2$ are suitable for this task. For a decisive choice more detailed simulation of the background with $\theta_\mu \rightarrow 0$ is needed.

It was shown earlier [11] that p_T is less efficient than θ_μ for signal extraction

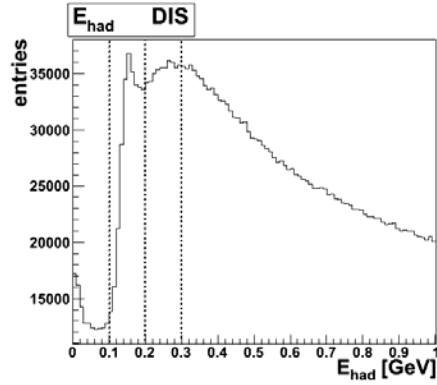


Fig. 14. Distribution over the recoil (hadronic) energy. Dotted lines indicate the applied cuts (see the text)

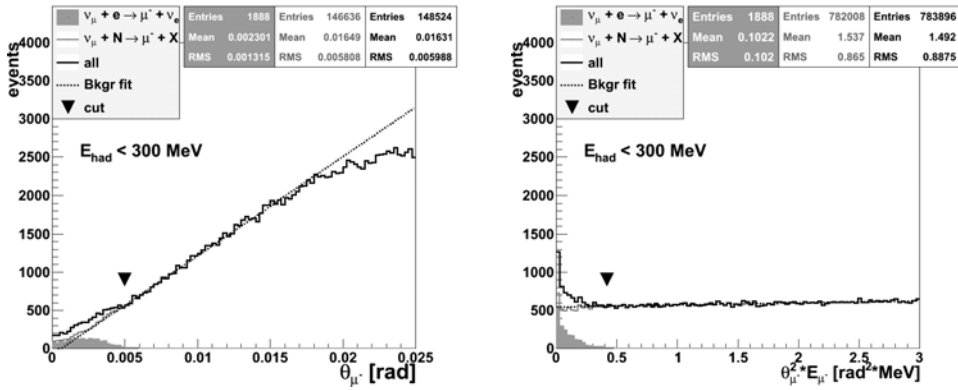


Fig. 15. “Measured” distributions over the indicated variables of the outgoing muons in the so called *poor* scenario (see the text). The leptonic events are filled with gray, the hadronic events are plotted in gray and the total spectrum is in black. The cut value is denoted by a black inverted triangle. Dotted lines indicate the background extrapolation

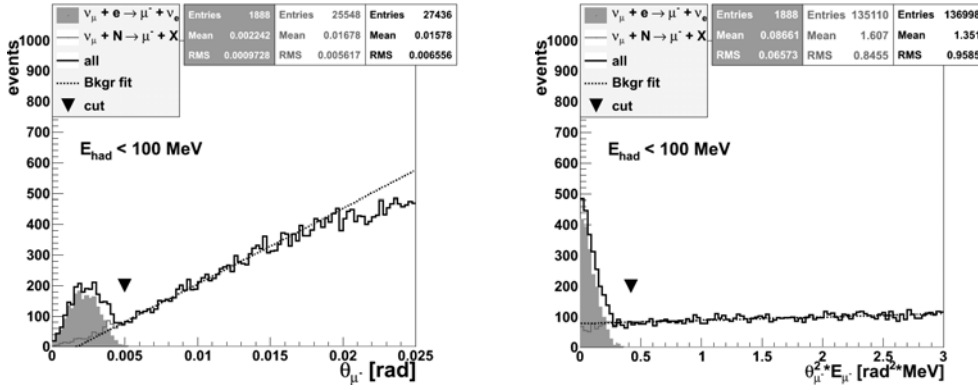


Fig. 16. “Measured” distributions over the indicated variables for the outgoing muons in the so called *best* scenario (see the text). The leptonic events are filled with gray, the hadronic events are plotted in gray and the total spectrum is in black. The cut value is denoted by a black inverted triangle. Dotted lines indicate the background extrapolation

4. CONCLUSIONS

It is feasible to use the quasi-elastic neutrino scattering off electrons for measuring the neutrino flux coming from the *neutrino factory* storage ring with a precision of a few *percent*. For a chosen resolution on θ_μ , E_μ and E_{had} , the angle θ_μ and the composite variable $E_\mu * \theta_\mu^2$ have similar discriminating power. The last one seems to have more flat distribution when $\theta_\mu \rightarrow 0$. The confidence on the measurement of E_{had} down to few tens of MeV is crucial for the selection.

Acknowledgements. This work has been supported in part by the European Union Research Executive Agency under FP7 Grant agreement No. 212372 and by the Bulgarian National Science Fund under contract No. VU-F-205/2006.

REFERENCES

- [1] Geer, S. *Phys. Rev. D*, 1998, **57**, 6989.
- [2] Bandyopadhyay, A. et al. *Rept. Progr. Phys.*, 2009, **72**, 106201, [arXiv:0710.4947].
- [3] See, for example:
 Mohapatra, R., P. Pal. *Massive Neutrinos in Physics and Astrophysics*. *World Sci.*, 2004;
 Gonzalez-Garcia, M.C., M. Maltoni. *Phys. Rep.*, 2008, **460**, 1;
 Dore, U., and D. Orestano. *Experimental results on neutrino oscillations*, e-print arXiv:0819.1194.
- [4] Abe, T., et al. *Journal of Instrumentation*, 2009, **4**, T05001.
- [5] Bardin, D., and V. Dokuchaeva. *Nucl. Phys. B*, 1987, **287**, 839.

- [6] International Design Study for Neutrino Factory Working Group, <https://www.ids-nf.org/wiki/FrontPage/Documentation?action=AttachFile&do=get&target=IDS-NF-002-v1.0.pdf>
- [7] Vilain, P., et al. (CHARM II Collaboration). *Phys. Lett. B*, 1995, **364**, 121.
- [8] Mishra, S. R., et al. *Phys. Lett. B*, 1990, **252**, 170.
- [9] See GENIE web site: <http://www.genie-mc.org>.
- [10] Andreopoulos, C., et al. *The GENIE Neutrino Monte Carlo Generator*, e-print: arXiv:0905.2517v1.
- [11] Karadzhov, Y. Poster No. 56 at NuFact2009, Chicago, July 20-25, 2009.